Comput Geosci (2007) 11:9–26
DOI 10.1007/s10596-006-9032-8

ORIGINAL PAPER

Geometric modelling and object-oriented software concepts applied to a heterogeneous fractured network from the Grimsel rock laboratory

Thomas Kalbacher · Ralph Mettier · Chris McDermott · Wenqing Wang · Georg Kosakowski · Takeo Taniguchi · Olaf Kolditz

Received: 3 April 2006 / Accepted: 21 September 2006 / Published online: 18 November 2006

Abstract Discrete fracture network simulations are computationally intensive and usually time-consuming to construct and configure. This paper presents a case study with techniques for building a 3D finite element model of an inhomogeneous fracture network for modelling flow and tracer transport, combining deterministic and stochastic information on fracture aperture distributions. The complex intersected fractures represent a challenge for geometrical model design, mesh quality requirements and property allocations. For the integrated and holistic modelling approach, including the application of numerical and analytical simulation techniques, new object-oriented concepts in software engineering are implemented to ensure a resourceful and practicable software environment.

Keywords fracture apertures · fractured network · geometric modelling · geostatistics · mesh quality · object orientation

T. Kalbacher · C. McDermott · W. Wang · O. Kolditz
Center for Applied Geoscience, University of Tübingen, Tübingen, Germany

R. Mettier · G. Kosakowski
Paul Scherrer Institut, Villigen PSI, Switzerland

T. Taniguchi
Graduate School of Environmental Science, Okayama University, Japan

T. Kalbacher (✉)
Center for Applied Geoscience (ZAG), Sigwartstr. 10, D-72076 Tübingen, Germany
e-mail: thomas.kalbacher@uni-tuebingen.de

1 Introduction

After long-standing research, understanding flow and transport processes in natural fractured rocks remains a challenging task. This is mainly due to the geometric complexity, the scale dependence, strongly varying fracture properties and the interaction of multiple-scale features and processes that influence the flow and transport characteristics of fractured rocks. Fields of applications include the oil industry, deep geological repositories for toxic or radioactive waste, utilisation of geothermal energy and CO_2 sequestration. Predictive modelling of flow and transport in fracture networks is vital for realistic long-term management of the systems in question.

A major step for fracture network development and application includes the conceptualisation and preprocessing of the input data. This comprises the design of the conceptual model, cleaning of the geometric data, meshing of the geometry in a quality that is adequate for the specific finite element (FE) model and methods to assign physical properties and parameters. The preprocessing is very often the most time-consuming task in the modelling chain, and the limited ability of specific software tools necessitates conceptual simplifications. In most applications, fracture network geometries must be strongly simplified, as only a limited amount of information about the actual network geometry is available. Determining the actual position of fractures in an *in situ* rock volume is possible only for major fractures on the scale of decameters and above [17], or otherwise for small laboratory-scale rock samples. Geological evidence, however, constantly reminds us that natural fracture networks do not show much similarity to simplified models, and are often dominated by millimeter aperture fractures running over lengths of centimeter to tens

of meters [43]. The increasing demand of more detailed, more complex, and therefore more realistic conceptual models for fractured networks requires the development of new methods to design and discretise the geometric model.

In general, two basic "end" concepts exist for the numerical modelling of fractured rocks: discrete fracture models and continuum models. Different types of discrete fracture models are described and applied first, e.g. by Brown and Scholz [8], Moreno et al. [41] and Tsang [50]. Some of the standard methods include simplifying the fracture network geometry to either an equivalent porous medium or a single fracture [34, 36, 41, 45]. Others combine the fracture network geometries to a network of tubes [4, 9, 16, 14], or as an ensemble of a few clearly determined and well-defined fractures [31, 37]. A holistic approach combining the benefits of discrete and continuum models is to use a hybrid approach [23] based on the architectural elements of the deposits being modelled, for instance the definition of geomechanical facies [39].

The influence of small-scale heterogeneities, like fracture surface roughness or fracture aperture variations, has been shown to be a significant factor affecting the flow and transport within fractures. In fracture network models, the individual fracture apertures may be considered as constant [12], or described with a geostatistical distribution, e.g. a lognormal distribution or fractal-based distribution [38, 42]. Such realistic-seeming fracture networks can be generated with statistical approaches, such as are applied by 'FracXP' software package from Golder Associates [15]. They can be conditioned to previously known information, such as fracture traces on the boundary surfaces of the studied rock volume, or borehole logs. Often, these generated fracture networks avoid sharp angles at fracture intersections, multiple intersections with small separations and generally numerically difficult geometries. This provides an advantage for the domain discretisation, but maybe oversimplifies the conceptualisation.

Most often, discrete FE models are used to deal with complex fractured network geometries. Some recent approaches include 2D fractures in 3D volume with power-law distributed fracture sizes [30, 42], or 2D fracture networks with power-law distributed fracture lengths [14]. Also, a combination of 1, 2 and 3D elements to model 2D fractures in 3D porous media can be applied [47]. The complexity of the conceptual model depends on the content and quality of the base dataset, the requirements of the modelling code, the actual requirements and constraints of chemical and/or physical processes and features under investigation. Additionally, the accuracy of the conceptual model depends on the quantity and quality of the computer-aided methods for the model design. A synchronized development of all these components is required to increase the potential geometric complexity and ensure the applicability of the FE model. A clearly structured and object-oriented software environment supports the task of such coordinated and balanced software developments. Here the procedures to set up a realistic and complex fracture network model for mass transport calculations taking into account processes on several scales is presented. This requires the following:

- Measurements of discrete fracture data and the model concept for application-oriented conceptualisation (Section 2).
- A well-organized code structure is needed which enables a transparent administration of the source code for a group of natural scientists and/or engineers (Section 3).
- Geometric model design: Robust calculations of the intersections between multiple fractures are used but the reliability of the results varies. Analyzing and cleaning of geometry is needed to ensure the suitability of the conceptual model (Section 4).
- Dedicated mesh generation techniques, which must take the fracture intersections as well as topologic and geometric relationships into account (Section 5).
- Physical assignments: The increasing demand for more detailed three-dimensional fracture network models as well as the permanent extension of models by introduction of new physical processes can lead to large mesh constructs, which are no longer visually controllable for manual parameter and property allocation. We suggest performing the management of these datasets, e.g. boundary conditions, by use of geometric information from the initial conceptual model (section 6).
- Information about the fracture aperture distribution: Fracture apertures can vary, and measured distributions are often not or only insufficient available for geostatistical procedures. However, the fracture aperture distribution needs direct linking to the finite element mesh (Section 6).

2 Dataset and model concept

The procedures described in this paper are demonstrated by using detailed experimental information gained from the excavation project at Nagra's Grimsel Test Site (Switzerland) [2]. In this project, comprehensive data has been gained on the fracture geometry and the flow and transport characteristics of a 2-m-long *in situ* section of a shear zone. Initially, a number of radionuclide transport tracer experiments were performed on the shear zone followed by impregnation of the fracture network with fluorescent resin. Subsequent overcoring parallel to the main flow direction, and extraction of the resulting large diameter cores enabled a

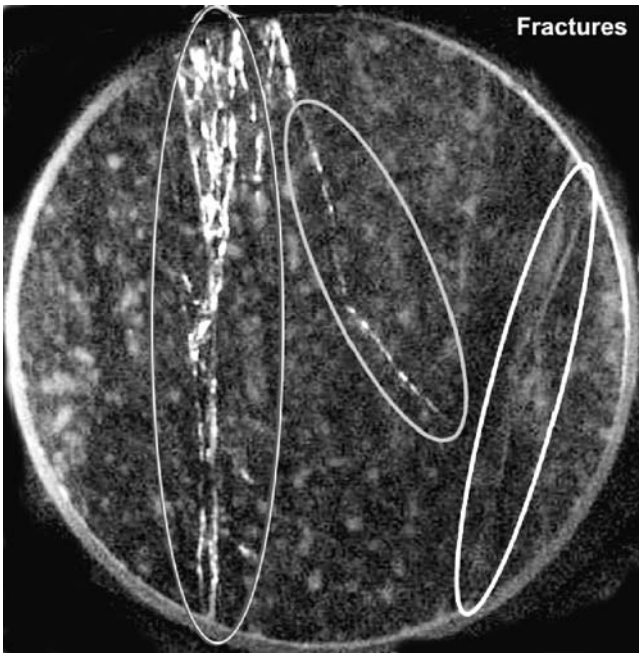

Figure 1 Ultraviolet photography of a core slices obtained from the excavation project (Ø ~ 30 cm). Located fractures are circled [40].

significant percentage of the rock volume involved in the flow and transport tests to be sliced and photographed in visible and ultraviolet light (figure 1). The resulting set of digital images presents a unique view of the interior structure of such a fracture network. From this dataset, a geometric model of the fracture network can be reconstructed. Although this is still a simplification, such a model shows a strong similarity to the actual fracture network, as far as positioning and dimensions of major fractures is concerned. Further small heterogeneities, such as fracture apertures, may also be extracted from the images, and adapted to the geometric model by geostatistical methods [40]. The appeal of performing numerical flow and transport calculations on such a model is obvious, but the near-realistic geometric properties also create significant difficulties as far as pre-processing is concerned.

2.1 Dataset: determination of fracture geometry

Sequential viewing of the cross-section images allows the three-dimensional geometry of the fractures to be determined [3]. The fractures were designed by the use of all images and the definition of 3–10 points for each visible fracture section. The best-fitting planar surfaces through each fracture point cloud define the spatial fracture geometry. In the studied rock volume, three major fractures can be identified, approximately parallel to the extracted core axis. Nineteen further large fractures can be extracted, providing a degree of interconnection between the three main fractures. Additionally, a large number of very small fractures and other small features (e.g. fracture-filling fault gouge) can be identified. These are, however, neglected in the model geometry because their extent and shape are not clearly identifiable due to the limited image resolution.

2.2 Overview of the geometric and physical model concepts

All modelling studies rely on a logical simplification of the system. Numerical methods can be used to predict the interaction of various physical processes. However, the more detailed the system is modelled, the more complex the solution procedure becomes and the more time-consuming are the calculations. Based on fracture network geometry measurements and aperture distributions [40], two scales of fracture network modelling are addressed.

1. The macro scale provides the three-dimensional representation of the 2D planes in 3D space. The fractures are approximated by triangular finite elements. In this way, the large-scale features of geometry and the interconnectivity of the fractures in the fracture network can be represented.
2. At the micro scale, different fracture apertures are mapped to material properties of individual triangular finite elements. Thereby, according to a certain estimated fracture aperture at a certain locality, the element representing that locality is mapped with a material property (in this case, permeability). At the micro scale, the relationship between the fracture aperture and the intrinsic permeability is given over the cubic law [55]. Using the value of hydraulic conductivity K (m s^{-1}), for the fracture elements, and groundwater head h (m), allows the hydraulic mass balance equation to be written as

$$S\frac{\partial h}{\partial t} - \mathrm{div}(K\,\mathrm{grad}\,h) = Q \tag{1}$$

where S is the storage (m), t is time and Q is the volume flux (m^3 s^{-1}). The solution of this equation using the finite element technique is covered in standard works such as [24, 26, 56]. Solving Eq. (1) provides the fluid head at each discrete node in the FE model, which then can be interpolated for the elements and converted into flow velocities v (m s^{-1}) in the elements.

The flow velocities are then used to derive the solution of the mass transport Eq. (2) [10].

$$\frac{\partial C}{\partial t} - \mathrm{div}(\mathbf{D}\,\mathrm{grad}C) + v\cdot\mathrm{grad}\;C = C_s \tag{2}$$

Here, C is the concentration of the compound (kg m^{-3}) under investigation and D represents the effective diffusion

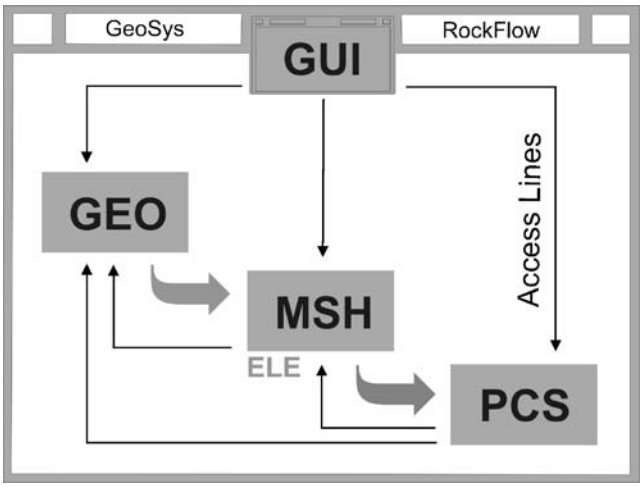

Figure 2 General concept of the object-oriented structure of GeoSys shows the four main object libraries and their access permission.

coefficient depending on the media ($m^2\ s^{-1}$) [21]. The term C_s refers to a source term (kg $m^{-3}\ s^{-1}$).

The transport of tracers in fractured media is governed by advective, diffusive, and dispersive mechanisms [18]. All these transport phenomena occur in the fractures and in the rock matrix. Several approaches allow the calculation of contaminant and heat transport in fractured media involving the diffusive exchange processes between water flowing through fractures and the rock matrix, known as matrix diffusion [44]. Analytical solutions can be applied to simple geometries such as single fractures or parallel fracture arrays [10, 32]. An excellent overview on analytical solutions for mass and heat transport analysis of porous media is given by Häfner et al. [22]. For the more complicated systems, analytical models can help to understand the interaction of the various processes, but numerical models are necessary for predictive modelling. For numerical analysis, stability criteria play an important role in ensuring the accuracy of the solution of the mass balance equations. One method for increasing the time efficiency and avoiding some stability problems is to include analytical solutions to describe diffusion-dominated processes.

Here, a hybrid approach to matrix diffusion is applied to remove the need to discretise the rock mass between the fractures. This significantly increases the efficiency of the modelling technique. The matrix diffusion of the tracer material is represented by an analytical source term, which takes into account the history of the concentration of the tracer passing the element in the fracture. Deriving from [22] the source term can be shown to be given by

$$C_s = \left[\sum_2^n \left[erfc\left(\frac{x}{2\sqrt{D_{app}(t_0 - t_{n-1})}}\right) - erfc\left(\frac{x}{2\sqrt{D_{app}(t_0 - t_n)}}\right) + erfc\left(\frac{x}{2\sqrt{D_{app}(t_0 - t_1)}}\right)\right]\right] 2AD_e \tag{3}$$

where n is the number of time steps prior to the current time step to be taken into account, A is the area of the fracture surface represented by the finite element node to which the source term is applied, D_e is the effective diffusion coefficient and D_{app} the apparent diffusion coefficient of the tracer in the matrix [21]. Using this approach, the matrix diffusion for non-sorbing and linear sorbing species can be calculated and is formulated here for a single-phase system. Details of the derivation and application of this solution will be given in a forthcoming report.

3 Software concept

This article gives a brief overview of the object-oriented procedures and implementations of the different objects. The illustrated methods and procedures of the next articles exemplify the need of a robust software concept to manage the use of new or improved software developments for FE modelling and preprocessing.

With the increasing requirements for the model design, comprehensive spatial data density with detailed property assignments and improved numerical approximations, object-oriented programming becomes increasingly important, especially in the context of complex natural environmental systems. A continual well-organized development of new methods for the fractured network model design, mesh generation and process data administration requires an efficient object-oriented code structure, which makes a transparent management of the source code for a group of natural scientists and/or engineers possible.

The concept of the GeoSys/RockFlow software development is based on object-oriented methods [26, 53] (figure 2) to achieve these aims. This guarantees a maximum reusability of all program components, helps to maintain the code structure, and enables continuous program development as well as an easy implementation of new functions.

3.1 Libraries

The object-oriented concept of GeoSys/RockFlow is the fundamental base for a stable interaction between geometric model design, meshing tools, visualisation, model admin-

istration and simulation. This assures flexibility and agility of the software development and allows fast rearrangement and optimisation, when new methods or processes are to be included. Four main object libraries, with geometric objects (GEO), mesh objects (MSH), process objects (PCS) and the graphical user interface (GUI), form the GeoSys/RockFlow software (figure 2). Unambiguous rules for the interacting data access of all four main object libraries are required to maintain these advantages.

The graphical user interface (GUI) is needed for 3D visualisation methods as well as for interactive control of geometric model design, meshing, physical assignments and process related administrations. Therefore, it is the only object, which can access to all object information.

The GEO has an internal topologic arrangement [11, 25] and includes data and methods for geometric points, polylines, surfaces, and volumes of the model domain. The geometric methods assign the options for the model design and its complexity. The GEO object is completely independent in its functionality and forbids the access to the other objects but allows unrestricted external access.

The mesh object (MSH) contains several mesh generators, mesh improvement methods, the mesh quality analyzing functions and uses GEO data structures as input. Consequently, it needs the full access to GEO data structures. The core component of the mesh object is the element object (ELE), described in the next section. The element data, such as geometrical and topological properties, as well as numerical operations of elements, like element matrix calculations and treatment of boundary conditions, are universally structured. The element object is also a fundamental entity for solving partial differential equations (PDE).

The process object (PCS) contains the numerical solvers, the equation system object, time step schemes, and all other process related methods. PCS can also be classified as the kernel of the simulator and it shows an internal object-oriented order [27]. The PCS needs access to MSH and to GEO. The central idea behind object orientation of processes is that the basic steps of the solution procedure – calculation of element contributions, assembly of equation system, solution of the equations system, linearisation methods and calculation of secondary variables – are independent of the specific problem [27, 28].

3.2 Element concept

The first step of finite element analysis is the domain discretisation and the construction of element meshes. The geometric element objects, one for each geometric element type (e.g. tetrahedra, cube, prism, etc.), are the basis of the element concept and their entities form the meshes. The finite element matrices for different PDEs are computed and the corresponding shape function is automatically selected according to its geometric element type. Finally, PCS objects assemble the equation systems for the problem type, in the case study presented here, the transport problems for fractured networks. The idea of the concept [53] is that specific, process-related information are introduced as late as possible to keep the software concept as clear and as flexible as possible.

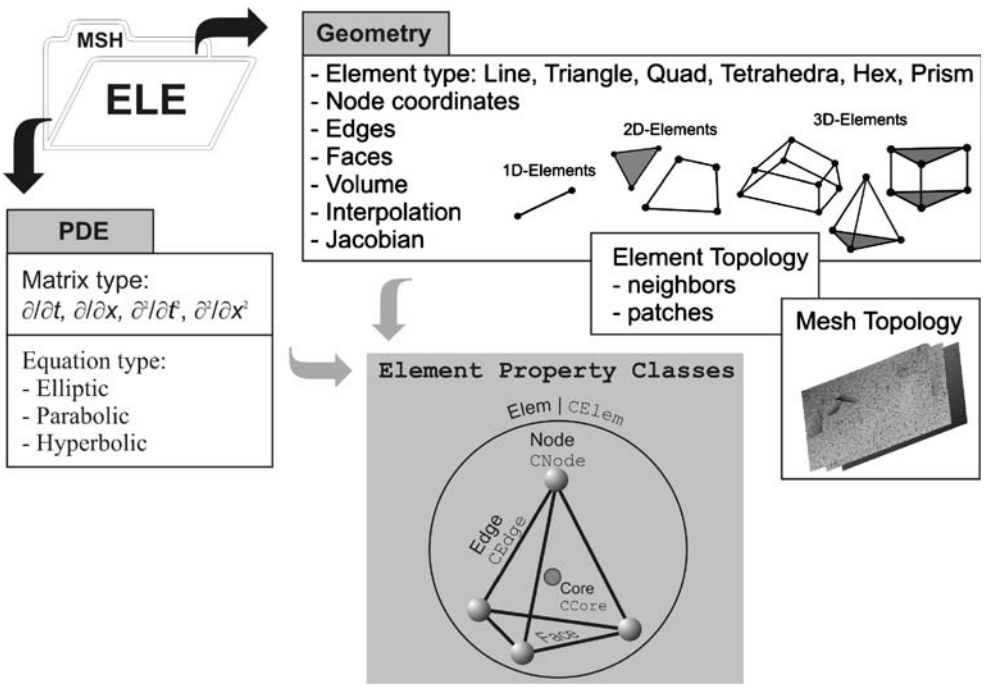

Figure 3 Geometry and PDE relation of the ELE object with the element property classes.

Figure 3 illustrates the concept of the element object. The element geometry includes the type specification (line, triangle, quad, tetrahedron, prism and hexahedron), the node coordinates, topological information of edges and faces, as well as volume quantification. Coordinate transformation functionalities are defined as geometric element properties, and neighbourhood relations of the elements define the element topologies, which are a function of the mesh topology.

The following four element property classes (figure 3) are designed to encapsulate all geometric and topological element information.

- The *CCore* class is abstracted as the base class of *CNode*, *CEdge* and *CElem*, and it contains common required data and methods.
- The *CNode* class is derived from the CCore class. The *CEdge* and *CElem* class are set as friend classes of *CNode* so that they can access to *CNode* private members directly. The *CNode* class provides the geometrical position of an element in real space and keeps the information which and how many elements use the particular mesh nodes. This node–element relationship contains very important information of the mesh topology, which is required, e.g. for mesh quality inspection, for extrapolation of Gauss point values to node values or for projecting element properties to nodes. It is organized as an own vector construct and the direct accessibility accelerates the topological methods.
- The *CElem* class represents an individual element of a mesh and it is derived from the *CCore* class. The node and edge class construct the element class. The *CElem* class is designed for the different geometric element types of lines, triangles, quadrilaterals, triangle-based prisms, tetrahedrons and hexahedrons.
- The *CEdge* class is derived from the CCore class. The edges construct the frame of a geometric element object and are frequently used as basic properties for mesh generation or mesh improvement methods. It is sufficient to use two nodes to form a geometric edge, but for higher-order finite elements, more points are required along an edge. In particular, the higher-order finite elements require edges through all computations. Therefore, we use a vector construct of *CNode* pointers as class member for all edge nodes. However, for node-based finite elements (i.e., linear interpolation), edges are only used to compute topological mesh structure and need not to be stored for later computations.

Element property numbers (element patch indices) are available for physical assignments and flux calculations. Depending on PDE type (elliptic, parabolic, hyperbolic,

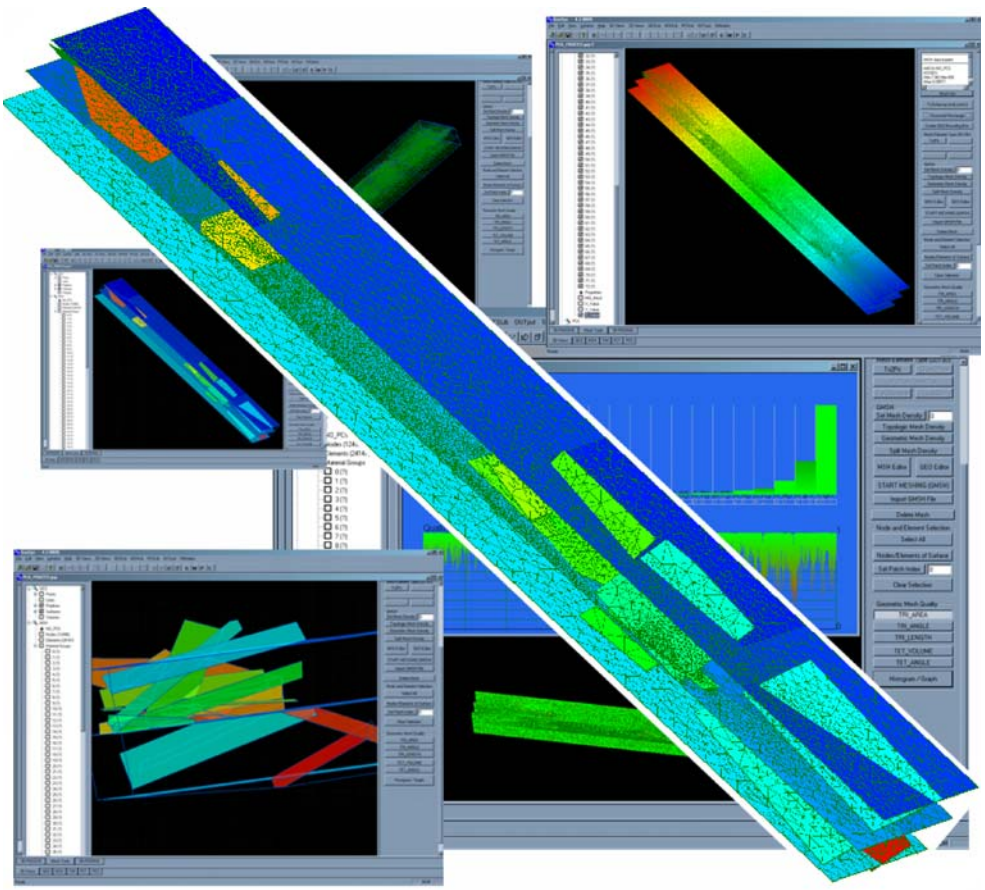

Figure 4 Visualization of the fracture network. Left: geometric input data visualization of polygons and surfaces. Top: view of mesh and result of a test run. Right: mesh quality analysis. Middle: triangulated network with patch index distribution.

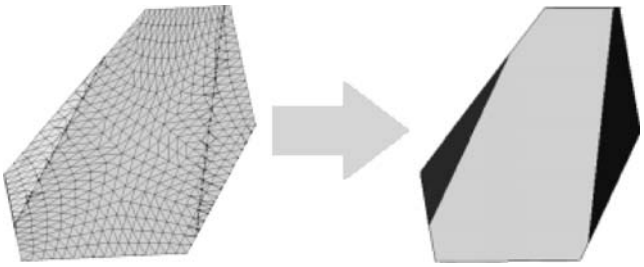

Figure 5 The original fracture plane is split into three polygons, which are then imported in GeoSys.

mixed), different first- or second-order differential terms can be evaluated ($\partial/\partial t$, $\partial/\partial x$; $\partial^2/\partial^2 t$; $\partial^3/\partial^3 x$). These differential terms are categorized in corresponding finite element matrix types: mass matrix, advection, dynamic, Laplacian matrix, tangential matrix and coupling matrixes. The major advantage of this approach is that element operations such as interpolations (shape functions) and derivations as well as tensor operations and Gaussian integrations can be conducted by considering the geometric element types only.

The presented object-oriented concept provides an efficient coding environment for geometric methods, mesh generation, mesh inspection and property assignment techniques. The following sections illustrate such procedures, which were essentially developed for the construction of the fracture network model.

4 Geometric modelling

The fractures extracted from the rock cores (see Section 2.1) provide the first geometric input data concerning fracture orientation and intersections. Subsequently, all fractures are approximated as planar surfaces. Next, intersections are calculated, followed by the segmentation of the surfaces into interconnected polygons. When dealing with a number of intersecting planar fractures, it is necessary to ensure a consistent geometry by checking the geometric and topological relationships of all geometric objects, such as points, polylines and surfaces, and to eliminate geometric conflicts. Modifications and extensions of the geometric input data are needed to make the data conform for mesh generation and available for the FE modelling (figure 4).

The following sections describe the procedures to build geometric model based on the simplified fracture geometry. Polygons have to be prepared to describe the model geometry, because these polygons describe the surface boundaries, which are required for mesh generation. The geometry of the conceptual model must be analysed and be

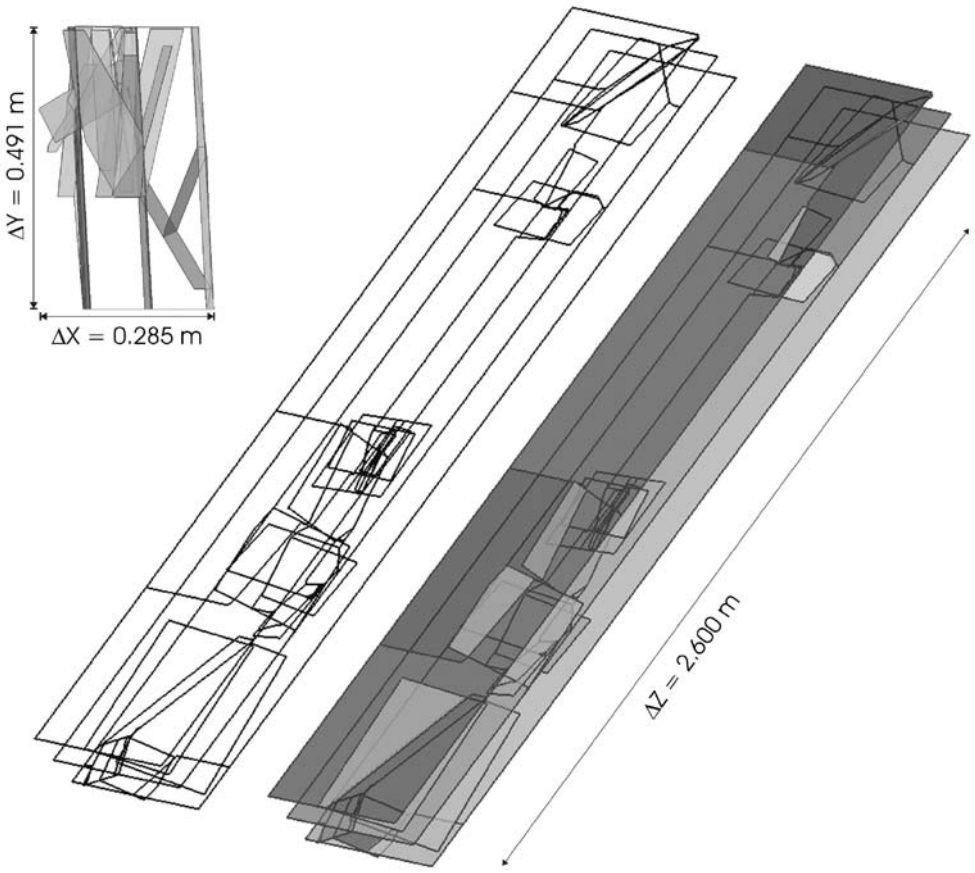

Figure 6 Geometric polylines and surfaces, which are needed to construct the fracture network model. Top left: *x*/*y* top view of the fracture network.

improved (cleaning) if necessary to ensure the applicability for mesh generation and the FE model simulation.

4.1 Intersections and polygon decomposition

Each plane surface of the fractures has to be subdivided into smaller units under consideration of its intersections with other surfaces. Some preprocessing of the dataset, e.g. the calculation of the intersection lines between the fractures, was done within the matrix and fracture interaction code MAFIC "Mesh" [35]. To apply further improvement techniques for the conceptual model, the intersection lines and segments of the planar fractures had to be reconstructed and combined to single polygons (figure 5). After all fracture planes have been split in this manner, the collected polygons are exported as a GeoSys geometry file.

4.2 Geometric data analysis and data cleaning

Geometric model quality problems are rooted in a variety of contributing factors that range from bugs in the preprocessing modelling system to errors of the data translation code. Data control and cleaning up of structure and precision are always needed to make the data functional for mesh generation and FE modelling. Consequently, complex fracture network models cannot be built without any user-controlled corrections and simplification to avoid errors in structure, precision and representation of reality. Structural problems include incoherent polyline orientation, fragmentary geometric input and non-defined or incorrect intersections. Structural errors can produce finite element meshes with intersected or not connected elements. This results in an unusable mesh for the numerical finite element model. Undesired effects are not attached fractures or fracture parts and consequent program crashes while solving the FE method problem. Precision requirements place limits on gaps between neighbouring geometric entities. Identical points should therefore be defined once by coordinates and the higher geometric entities by the point identification number. The model designer must balance the accuracy of numerical models with the amount of geometric information required. Precise fracture network models require complex and large data structures to define them, and simplifications are necessary to administrate and ensure the accuracy. Errors of reality representation can allow a model to run but the results are unrealistic due to physical limitations. Manual simplifications as well as automatic modulation procedures can cause such errors in the intersected areas of fracture network models.

4.2.1 Analysis of geometry

The fracture network of the case study presented consists of 233 points, 74 polygons and, consequently, 74 surfaces,

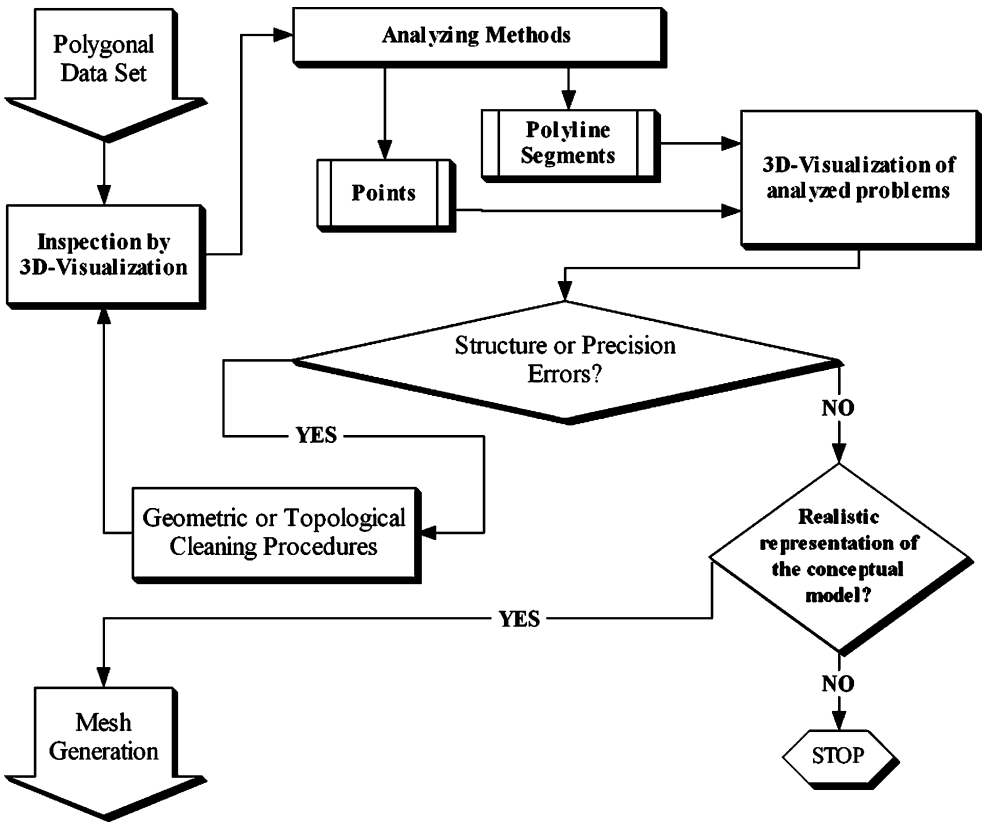

Figure 7 Procedure to prepare the conceptual model for mesh generation and FE model application. It is an iterative procedure with interaction of cleaning processes, data analysis and 3D visualization.

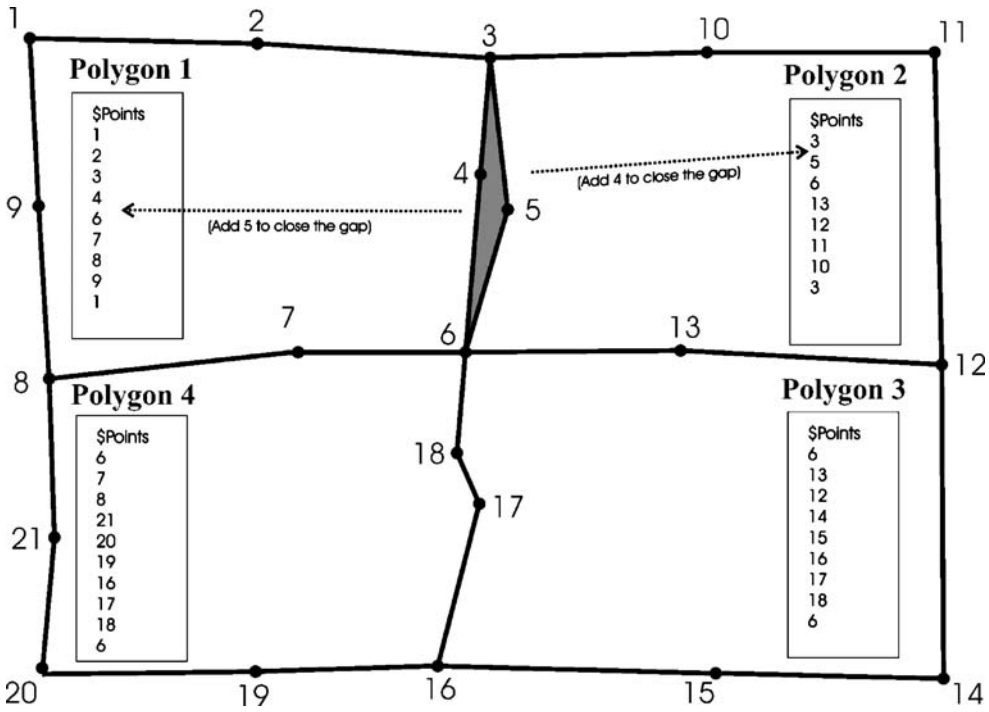

Figure 8 Example of an inconsistent polyline definition: Polygon 1 uses only Point 4 and Polygon 2 only Point 5. Both polygons must be corrected to close the gap (grey triangle.) The correction of only one polygon definition would produce another structural error by an undefined intersection.

which illustrate the 21 plane fractures (figure 7). The graphical user interface of GeoSys offers several tools for the geometric data analysis, and provides an OpenGL-based 3D visualisation (figure 4) of the fractured network data (geometry, mesh, properties, results) from any angle and position and allows image processing.

The 3D visualisation of geometric objects is an important tool to analyse the geometric input data (figure 6) and assists to localize accuracy and structural problems like missing geometry, gaps in polylines and gaps between polylines or surfaces. After analysing the consistency of the geometric data, it is necessary to prepare the geometry for the mesh generation. The user should have a clear idea how the mesh density distribution should look like, and which minimum and maximum element sizes are needed. The minimum is limited by the maximum of usable mesh size and mesh refinement. This defines the maximal geometric precision. The improvement of the geometric model is mostly an iterative procedure of geometric analysis and cleaning. Figure 7 illustrates the importance of efficient working analysis tools and cleaning procedures in combination with visualisation.

4.2.2 Data cleaning

A geometric searching algorithm examines the distances between points. This is important because small geometric point distances need local mesh refinement to ensure a certain mesh quality. This can increase the mesh size (number of nodes/elements) in a way that matrices for FE model simulation cannot be built up on standard computers or that the robustness limit of mesh generators is exceeded. In such cases, further geometric cleaning and simplifications are required. Should points be identified which are to close to one another, a merging tool can mark, display and combine those points that have smaller Euclidean distances than the user-defined tolerance. A further cleaning method is founded on geometric and topological techniques using the segment length of the polylines. Important information is the minimum and maximum length of all segments. The automatic "set length" function adds and removes points along the polyline segments with reference to the min/max length setting. This automatic function can distort the model domain as well as the automatic merging method, because curvature tests and other shape analysing methods are not implemented yet. However, both methods together are a useful tool to localize accuracy problems and help to improve the geometric data for mesh generation.

The GUI enables automatic cleanups as well as direct geometric data control using editors. In the case of this fracture network model, the GUI was needed to analyse the geometric input and to make some corrections to fix inconsistent polyline definitions (figure 8), to close gaps between polylines or surfaces, to modify or delete surfaces with acute angles (figure 9), and to merge points for a larger minimum distance of neighbouring points.

After cleaning the geometry, it is possible to add further geometric entities, e.g. to position boundary conditions or source and sink terms. Such extended geometries are usually transmitted geometric parts of the conceptual model

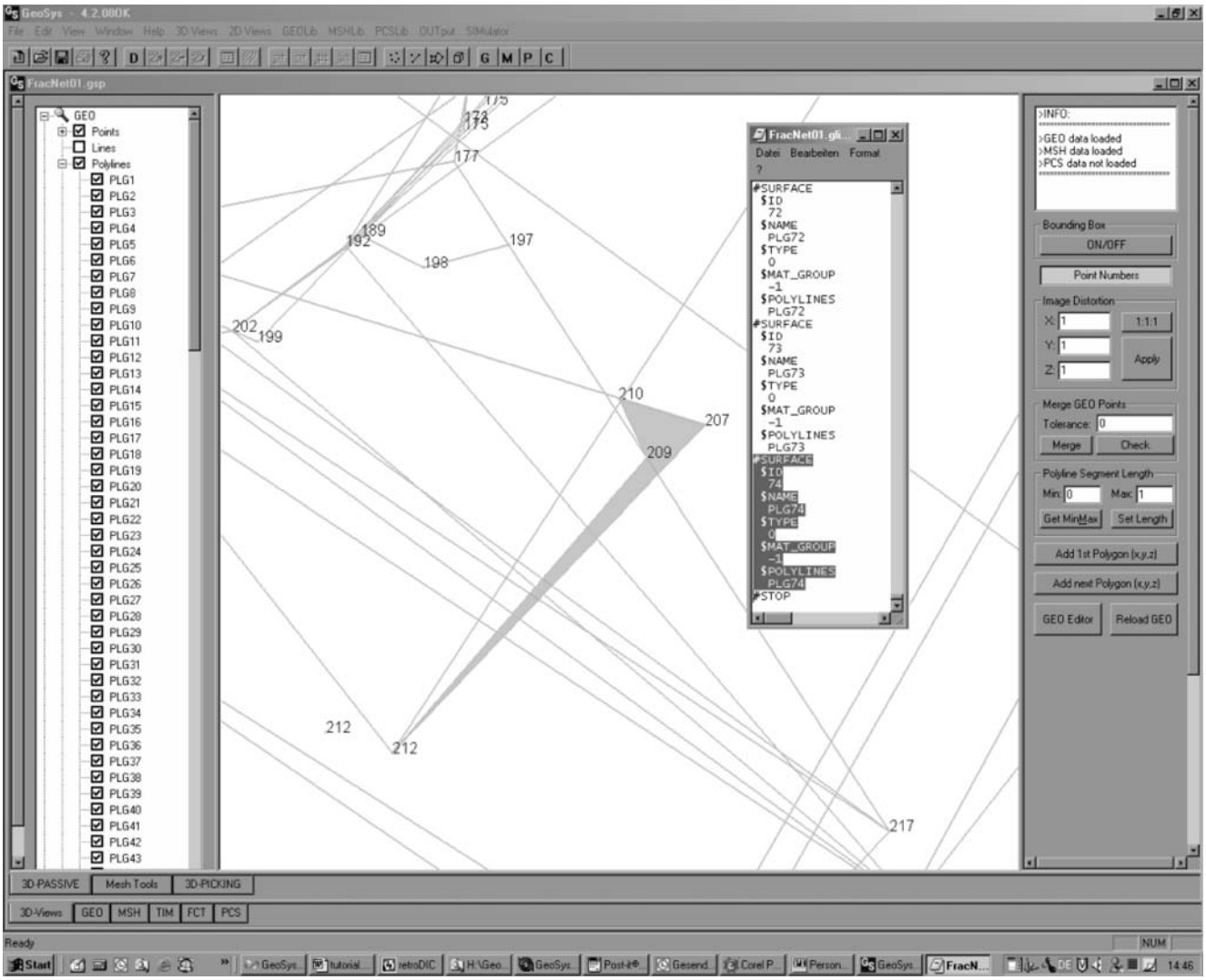

Figure 9 Surface with acute angle – This surface was deleted because of its shape and small relevance (small size and marginal position) for the model.

and should be included as late as possible. The insertion would be possible before cleaning as well, but this produces additional work for analyzing and modifying of these geometric entities after each cleaning procedure. In Section 6, more surfaces are introduced for boundary conditions using the point, polyline and surface editors together with the 3D visualisation for visual support and control.

5 Mesh generation

Meshing is an integral part of the FE model analysis process. The quantity and quality of the finite elements influences the accuracy, convergence and speed of the fractured network model solution. More importantly, the time it takes to create a mesh model is often a significant portion of the time it takes to get results from an FE method solution. Therefore, the more user-friendly and automated the meshing tools, the less time consuming is the evaluation of the appropriate settings for an optimal mesh density distribution.

The MSH includes objects of fundamental algorithms and mathematics for meshing and remeshing, independently usable but specifically designed for the class of geometric data. It provides structured and unstructured tetrahedra-, hexahedra-, prism-, rectangle- and triangle-mesh generators and quality analyzing tools. Structured meshes would offer a more direct control of size and shape of elements but are less flexible in fitting the domain along complex fracture intersections than unstructured mesh generation. The used mesh generator is based on Delaunay Triangulation [49] performed by GMSH [20]. The procedure can be classified in the following steps:

- First, meshing of a box defined by boundary nodes resulting from the discretisation of the surfaces is undertaken.

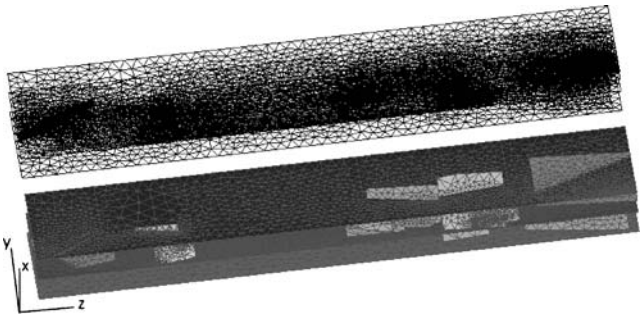

Figure 10 Triangulated fracture network (top) and patch indices (bottom). Elements of the same single surface have the same patch index and therefore the 73 surfaces created 73 different patch indices.

- Second, insertion of all the nodes on the surfaces based on the Bowyer–Watson algorithm [7, 54] for an initial triangulation, and a boundary reinstallation to keep all the edges of the surfaces to be present in the initial mesh.
- Third, the displacement of all the objectionable triangles and finally the insertion of new nodes by the Bowyer–Watson algorithm until the characteristic size of all triangles correspond with the mesh density description.

5.1 Mesh density

The density of the created mesh follows specific element size definitions (edge length of triangles) at points of the bounding segments. An element size definition at each geometric point is essential before starting the mesh generation. The element size allocation must take user-defined density distribution as well as the geometric required element sizes into account. A very small segment in the boundary needs a region of small elements in the surrounding area of the segment to ensure an appropriate mesh quality.

The user specifies at first a global maximum element size for all points and starts an automatic mesh density adaptation. The smaller the predefined specific element sizes, the less mesh refinements are necessary and the more homogeneous is the mesh of the fractured network model. GeoSys/RockFlow offers a topological and a geometrical optimisation technique. The geometric method takes only the Euclidian distance per point to all neighbouring GEO points into account and sets the minimum distance of the closest neighbour point as specific element size for the analysed point. The topological method calculates the Euclidian distance along topologically connected and neighbouring entities and sets the minimum distance as the specific element size. This might be critical if two or more not interconnected polyline segments are very close together. The specific element size is only changed when the calculated value is smaller than the predefined elements size value. Both optimisation techniques can lead to heterogeneous mesh constructs if the conceptual model shows alternating geometric complexity. Strong mesh refinements can be avoided by downscaling the global maximum element edge size, to achieve a more homogenous mesh and to prevent oscillating results for the mass transport modelling. Here, the needed process related element edge size is <0.10 m (numerical stability criteria) but the global defined maximum edge length is 0.05 m and produces in combination with the geometric optimisation method a less heterogeneous mesh with appropriate refinements around the fracture intersections of the $2.6\times0.5\times0.3$ m fracture network.

5.2 Meshing procedure

After mesh density definition and the selection of the applicable surfaces, the mesh generation can be started. The mesh consists now of 12,865 nodes and 24,840 triangular elements (figure 10). The minimum/maximum edge lengths are 7.96×10^{-5} and 0.085 m, and the average edge size is 0.2 m. The extreme minimum is the result of one intersected area where it was needed to place several points close to each other because of reality representation and structural uniqueness. In this case, fractures that were lying almost parallel would be incorrect connected.

The mesh is now refined in all areas where it is geometrically necessary. This should ensure an adequate mesh quality but must be analysed (see Section 5.3). The elements of each single meshed surface have the same element property numbers, which belong to the element object and which are mainly used for material group assignments and controllable within the GUI. Therefore, the 73 meshed surfaces, which construct the fractured network, produce 73 patch groups (figure 10).

5.3 Mesh quality

For the accurate calculation of the processes to be evaluated, the required mesh quality is actually also dependent on the process being considered. This makes it difficult to use geometric quality criteria alone before solution to evaluate the quality of the mesh for the process. There are available techniques that combine both the geometric quality of the mesh elements and the process solution procedure, the so-called solution-based computable error estimates (e.g. [6]). However, they are still under development for finite element analysis.

There are several ways to compute geometric quality of individual elements and to quantify the overall quality of a mesh [5]. In this paper, three elementary criterions for triangular elements have been applied. The fundamental principle is that equilateral triangles have the best possible

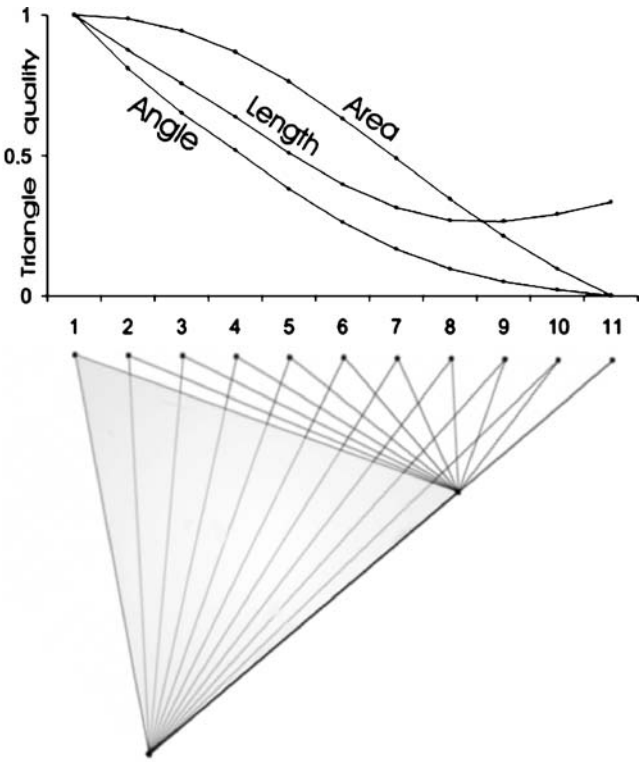

Figure 11 Length, angle and quality criteria for each triangle. The upper vertex of the grey equilateral triangle is moved by 10 steps horizontal to the right side.

element shape, and therefore the ideal number of elements linked to one node is six. The geometric quality can be expressed for triangular elements as

- LengthCriterion:

$$Quality_{\text{Lengh}} = \frac{\min\left(|\overrightarrow{e_1}|, |\overrightarrow{e_2}|, |\overrightarrow{e_3}|\right)}{\max\left(|\overrightarrow{e_1}|, |\overrightarrow{e_2}|, |\overrightarrow{e_3}|\right)} \tag{4}$$

- Angle Criteria:

$$Quality_{\text{Angle}} = \frac{\min(\alpha, \beta, \gamma)}{\max(\alpha, \beta, \gamma)} \tag{5}$$

- Area Criteria:

$$Quality_{\text{Area}} = \frac{4\sqrt{3}A}{|\overrightarrow{e_1}|^2 + |\overrightarrow{e_{21}}|^2 + |\overrightarrow{e_{31}}|^2} \tag{6}$$

The length criterion (4) is the relation of shortest and longest edge of the triangle $\left(|\overrightarrow{e_1}|, |\overrightarrow{e_2}|, |\overrightarrow{e_3}|\right)$, which is obviously one in the equilateral case just as well as the angle criterion (5), which is the ratio of the smallest to the largest angle (α, β, γ). Finally, the area criterion (6) compares the area A with the length of the edges $\left(|\overrightarrow{e_1}|, |\overrightarrow{e_2}|, |\overrightarrow{e_3}|\right)$, and is one for the equilateral triangles.

Figure 11 shows a comparison of the three triangle quality criterions. Starting with an equilateral triangle (grey triangle), the top left point with number 1 is moved along a horizontal line to the right side. Through this, we produce 11 triangles with decreasing quality until the triangle is completely distorted. For all 11 triangles, the quality criterions are calculated and displayed in a graph exactly over the moved top vertex of their corresponding triangles. The angle criterion is most sensitive for the upper quality range. Then the three graphs show nearly the same gradient. For the low quality range, the area criterion has the steepest gradient and therefore the most sensitive performance. The length criterion shows a divergent behaviour for triangles of lower quality (<0.35) where the quality factor starts increasing while the element quality is decreasing. These criteria are implemented within the GUI. The three-dimensional visualisation shows the spatial distribution of mesh quality (figure 4, right). This helps to localize critical areas of mesh quality (figure 12), but faces of completely distorted elements are invisible. Therefore, it is necessary to visualize the mesh quality of each element in a diagram (figure 12). An additional and maybe most important overview of the mesh quality distribution are given by histograms, which are displayed together with the element quality graph (figure 12).

Such geometric factors are not a guarantee for sufficient mesh quality for any physical processes. However, in combination with rule-based adaptive time step calculations they assist in appraising the usability of the mesh for the FE model application. Due to the sensitive performance in the low quality range of the fracture network mesh, we choose the area criterion to analyse triangles with a quality below 0.5 to extract and locate potential critical areas. First, we located poor elements along intersections (figure 12), and improved the mesh by manual geometric input corrections and refined remeshing. After the improvement, the mesh of the fractured network shows an adequate quality distribution but still some single poor elements (figure 12, minimum of lower diagram). These elements are due to acute angles of surface boundaries at fracture intersections, since the fracture geometry was not more simplified to avoid unwanted fracture linkage.

6 Physical assignments

The demand for more detailed and complex fracture network models as well as the task to extend the model by introducing new physical processes can lead to complex mesh constructs, which are no longer visually controllable for manual parameter and property assignments. User-defined management of these datasets has to be performed within a geometric environment, which excludes the finite

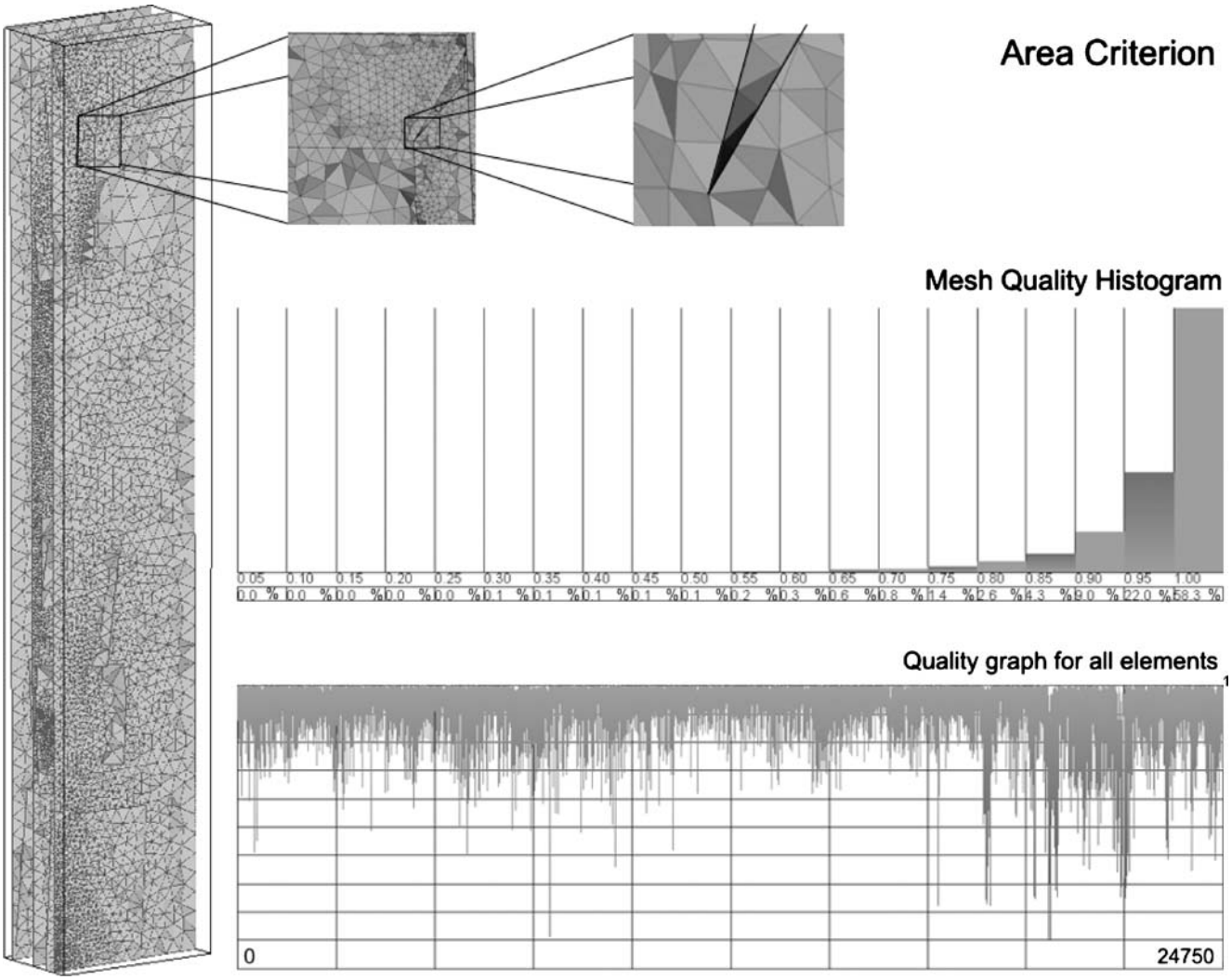

Figure 12 Spatial distribution of the area criterion (left) and an example of typical poor element quality (zoomed dark grey/black triangles) along fracture intersections (top). Histogram (middle) and graph (bottom) of the area criterion.

element mesh. Physical assignments are declared in the PCS object and are linked with the appropriate entities of the GEO object. Automated functions connect the information of MSH and PCS by using the geometric input data.

6.1 Node properties

The boundary conditions for the groundwater flow and mass transport model need specifications of hydraulic heads and concentrations, static or time-dependent, as well as the geometric locations for these conditions. Numerically, all locations for boundary conditions consist of a set of mesh nodes. As the complexity of the model increases, it may often become impossible for the user to visualize and assign node properties correctly. Therefore, the boundary conditions can be geometrically defined by the basic and initial geometric entities, e.g. points, polylines and surfaces. Here, the user simply selects the surfaces (figure 13) and defines the physical parameters, such as concentrations or hydraulic heads. A searching and allocation algorithm selects the appropriate mesh nodes and links them with the boundary condition object (figure 13). The following three major steps describe the applied procedure:

- Triangulation of the surfaces for the boundary conditions, with less (the more elements, the more time-consuming) but not distorted elements (because of robustness and reliability).
- Calculation of the geometric accuracy to calibrate the search algorithm. Only with a correct calibration is it possible to find exactly all points along the surface.
- Searching all nodes, which lie inside or on the edge of the triangulated surface. This is carried out via an angle sum calculation and/or area comparison: Connecting the point with the edges of a triangle produces three extra

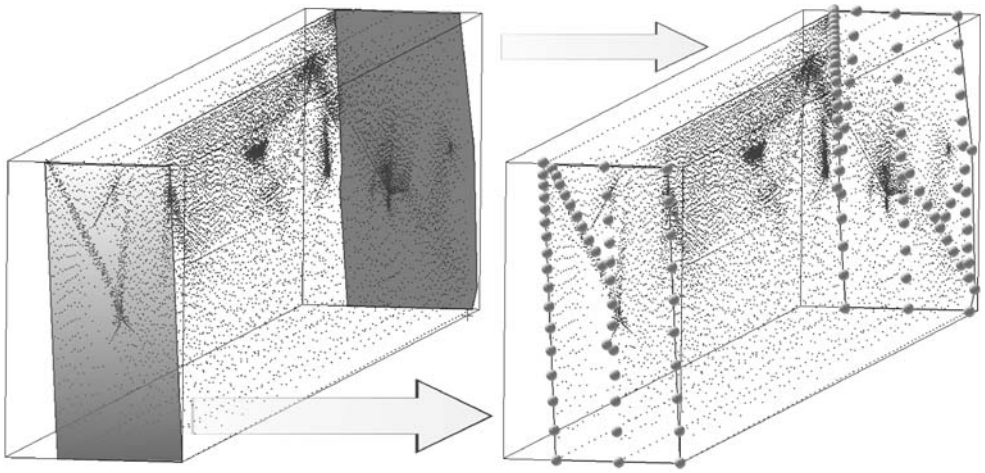

Figure 13 Surfaces (grey planes) are used to place boundary conditions (left). A search locates the mesh nodes for boundary condition setup (right).

triangles. If the point is inside, these three triangles altogether should have the same area as the base triangle, and the sum of their interior angles (angle of the common point) is 360°.

The advantage of physical assignment by basic and mesh-independent geometric entities is their fast creation. However, visual control is still very important to ensure the reliability.

6.2 Element properties

The assignment of heterogeneous material properties for fractures is done by directly connecting the material property parameters with the individual elements. In this case study, the fractures have variable apertures which are coupled with the transmissivity by the cubic law.

Several authors investigated the detailed structure of fracture surfaces, e.g. Brown and Scholz [8]. To reproduce the fracture roughness, i.e. the topography of fracture surfaces, different methods have been employed such as stochastic and fractal approaches [1, 19, 29, 38, 41, 52]. Fracture roughness effects the hydraulic conductivity of the fractures [33]. Fracture flow is divided into parallel and non-parallel motion by a critical value of roughness. Consequently, the specific geometry of a fracture (i.e., the distribution of the fracture aperture) influences its hydro-mechanical characteristics. This phenomenon is called flow channelling [51], and is taken into account in this modelling approach.

Geological evidence shows that fracture apertures are often spatially correlated, with an underlying lognormal distribution [13], causing a significant tailing in the breakthrough of solutes [40]. Geostatistical analysis, foremost the use of variograms, can provide a perception of the spatial distribution observed. If any actual apertures have been measured, an experimental variogram can be calculated from the data. A model variogram can then be fitted to the experimental one. This model variogram can be used to simulate any number of equivalently distributed aperture patterns by, e.g. sequential Gaussian simulation [46]. The patterns can be additionally conditioned to other measurements. They can be used in a Monte Carlo approach to investigate the effect of varying apertures on transport [40], or to recreated plausible aperture distributions in other models where no measurements on the actual apertures are available.

A simple tool enables the user to generate geostatistically distributed aperture values for model geometries consisting of planar, or near planar, fractures, discretised in 2D triangular elements. It makes use of the statistical program R [48], and therein mainly of the geostatistics package gstat [46].

The following requirements must be met:

- The fracture network geometry must consist of separable individual fractures, which either are of planar nature, or can be transformed (projected, warped, etc.) to planar form.
- The finite element mesh should consist of triangular elements.
- R 2.0 for Linux and the corresponding gstat package for R.

After the polygonal model geometry is loaded, the following steps are performed:

- Obtain the parameters which define the model variogram.
- If necessary, separate the fracture network into individual planar fractures.
- Create three R input files for each fracture (nodes.dat: consisting of the mesh vertices for each element (2D); centers.dat: which contains the center of mass for each element; rvario.r: the R script tailored to the calculation for each fracture).

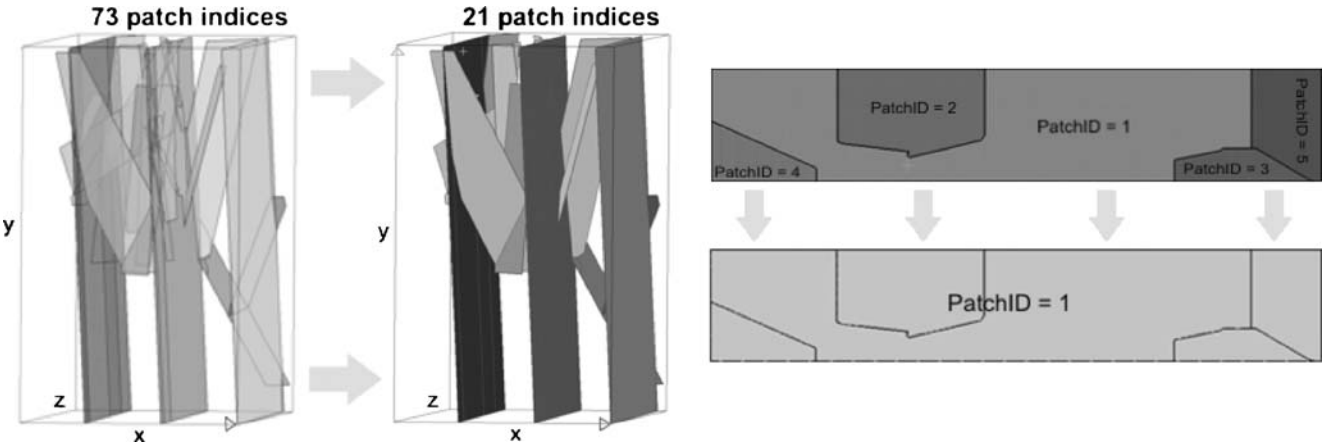

Figure 14 Merging of the patch indices for one fracture (right) and for the all fractures of the network (left).

- Call R, with the necessary options to execute rvario.r and return an output file, apert.dat, containing the aperture values at each of the element centers.
- Read apert.dat and assign each model element with the calculated aperture.
- Return the resulting model parameters to the patch object.
- Write the patch object out in a material file for distributed elements property data.

For the task of separating the individual fractures, element property indices are required to identify the element groups of each planar fracture (Section 6.3). The elements and vertices of each planar fracture are individually passed to the R input file generator together with the parameters, which characterize the variogram. This is done to ensure that intersecting fractures do not necessarily exhibit similar apertures near the intersection line, merely because their separation is small.

6.3 Simulation

The 73 patch groups (figure 6) represent the 73 surfaces, which were needed for the geometric discretisation of the fracture network model. The input is provided in form of a

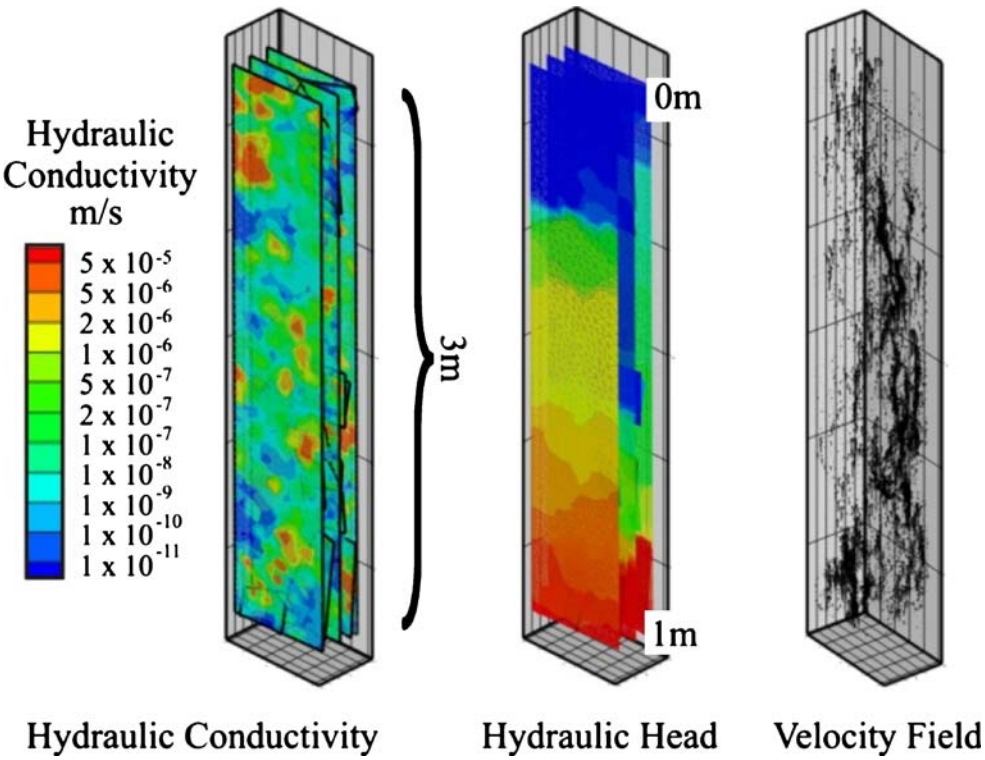

Figure 15 Permeability mapping and hydraulic results for the Grimsel shear zone.

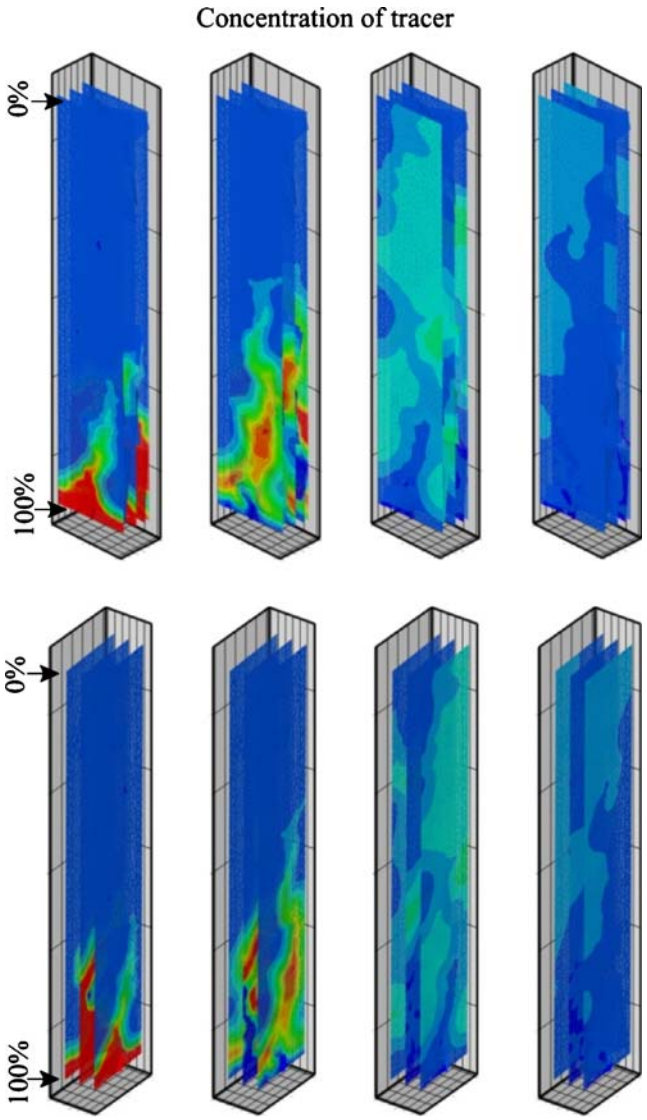

Figure 16 Tracer transport results with matrix diffusion for the Grimsel shear zone.

GeoSys MSH file, with a patch index for each element containing the element affiliation with a planar fracture. Therefore, it is necessary to merge all patch index groups, which belong to the same surfaces (figure 14).

After converting this arranged MSH file, now with 21 patch index groups (figure 14), to a GeoStatFrac file, the necessary parameters for the variogram model can be provided. The output is provided as a GeoSys material file (value per element), where additional material parameters such as aperture or transmissivity are related to element numbers. Figure 15 shows one realisation of a permeability distribution after such a geostatistical procedure.

Now, the geometric modelling – with model design, mesh generation, mesh analysis and the particular physical parameter assignments – is completed and the model can be applied for numerical simulations. Based on these results, experimental results can be analysed to determine the factors dominating the flow and transport characteristics of the shear zone material.

Using the procedure described above, figure 15 illustrates the mapping of the hydraulic conductivities onto a 3D representation of the investigated Grimsel shear zone, the solution of the heads according to Eq. (1) and the derivation of the velocity field. Figure 16 presents the solution of the transport equation with the inclusion of the matrix analytical solution Eq. (3) as a source term. Here, the initial transport results for four different time steps and from two different viewpoints are illustrated.

7 Conclusion

This paper presents necessary preprocessing steps to set up an FE model that allows calculation of advective and diffusive (dispersive) transport in realistic fractures, combined with slow diffusion of solutes into a porous rock matrix adjacent to the fractures and equilibrium sorption processes in the rock matrix. The methods and modelling assumptions can be tested on hand of a unique dataset comprising the internal geometry of a relatively large part of a shear zone in the Grimsel rock laboratory ($2.6 \times 0.5 \times 0.3$ m) and the results of real *in situ* transport experiments. To evaluate the results, numerous realisations of the fracture geometry based upon different geostatistical realisations of the measured fracture aperture distribution require a great deal of automation of the pre-processing tools. Due to the geometrical complexity of modelling fracture networks, it is necessary to have geometric and meshing tools capable of providing accurate geometric model design, domain discretisation and the spatial parameter assignments. The graphical user interface presented in this paper is able to show the user all required information (3D visualisation, diagrams, graphs, tables, etc.) and provides the interactive tools to administrate and revise the data. The complete object-oriented software concept must present a clear organized structure to maximize the reusability and flexibility of the source code for timesaving software engineering. In the case of the fractured network model presented, these capabilities are especially important because a large number of spatially and temporally, stochastic or deterministic distributed model properties are required.

Acknowledgements The authors want to particularly thank Nagra in Wettingen, Switzerland (http://nagra.ch, http://www.grimsel.com), and JAEA in Tokai, Japan (http://www.jaea.go.jp), which enabled the access to the cores themselves and provided the dataset from the excavation project as well as the images of the cores. Ralph Mettier

thanks Bill Dershowitz and Golder Inc. for providing him with an academic license for their FracXP software package. (http://fracman.golder.com/). The funding of the Deutsche Forschungsgemeinschaft (DFG) for further development of fracture network models under grant (MCD113/1-5) is gratefully acknowledged. Furthermore, we thank the BMBF for funding our developments of coupled numerical models for C:HM transport processes (02C1295)

References

1. Acuna, J.A., Yortsos, Y.C.: Application of fractal geometry to the study of networks of fractures and their pressure transient. Water Resour. Res. **31**(3), 527–540 (1995)
2. Alexander, W.R., Ota, K., Frieg, B.: The Nagra-JNC *in situ* study of safety relevant radionuclide retardation in fractured crystalline rock. Nagra Technical Report 00-06. Nagra, Wettingen, Switzerland (2003)
3. Baraka-Lokmane, S., Liedl, R., Teutsch, G.: Comparison of measured and modelled hydraulic conductivities of fractured sandstone cores. Pure Appl. Geophys. **160**, 909–927 (2003)
4. Berkowitz, B., Scher, H.: Anomalous transport in random fracture networks. Phys. Rev. Lett. **79**, 4038–4041 (1997)
5. Bern, M., Epstein, D.: Mesh Generation and Optimal Triangulation. Report CSL 92-1, Xerox Corporation, Palo Alto Research Center, Palo Alto, CA, 94304 (1992)
6. Berzins, M.: Solution-based mesh quality indicators for triangular and tetrahedral meshes. Int. J. Comput. Geom. Appl. **10**(3), 333–346 (2000)
7. Bowyer, A.: Computing Dirichlet tessellations. Comput. J. **24**(2), 162–166 (1981)
8. Brown, S.R., Scholz, C.H.: Broad bandwidth study of the topography of natural rock surfaces. JGR, J. Geophys. Res. B **90**(14), 12.575–12.582 (1985)
9. Cacas, M.C., Ledoux, E., De Marsily, G., Tillie, B., Barbreau, A., Durand, E., Feuga, B., Peaudecerf, P.: Modeling fracture flow with a stochastic discrete fracture network: calibration and validation 1. The flow model. Water Resour. Res. **26**, 479–489 (1990)
10. Carslaw, H.S., Jaeger, J.C.: Conduction of Heat in Solids. Oxford University Press Oxford, UK, (1959)
11. Chen, C.: Integrating GIS methods for the analysis of geosystems. PhD thesis, Center for Applied Geoscience, University of Tübingen (2006)
12. Cvetkovic, V., Painter, S., Outters, N., Selroos, J.O.: Stochastic simulation of radionuclide migration in discretely fractured rock near the Äspö Hard Rock Laboratory. Water Resour. Res. **40** (2004)
13. de Dreuzy, J-R., Davy, P., Bour, O.: Hydraulic properties of two dimensional random fracture networks following a power law length distribution, 2. Permeability of networks based on lognormal distribution of apertures. Water Resour. Res. **37**(8), 2079–2095 (2001)
14. de Dreuzy, J.-R., Darcel, C., Davy, P., Bour, O.: Influence of spatial correlation of fracture centers on the permeability of two-dimensional fracture networks following a power law length-distribution. Water Resour. Res. **40** (2004)
15. Dershowitz, W., Lee, G., Geier, J., La Pointe, P.: FracMan Interactive Discrete Feature Data Analysis Geometric Modelling and Exploration – User documentation (1995)
16. Dershowitz, W., Fidelibus, C.: Derivation of equivalent pipe network analogues for three-dimensional discrete fracture networks by the boundary element method. Water Resour. Res. **35**, 2685–2692 (1999)
17. Fisher, M.K., Wright, C.A., Davidson, B.M., Goodwin, A.K., Fielder, E.O., Buckler, W.S., Steinsberger, N.P.: Integrating fracture-mapping technologies to improve stimulations in the Barnett Shale. SPE Prod. Facil. 85–93 (2005)
18. Freeze, R.A., Cherry, J.A.: Groundwater. Prentice-Hall Englewood Cliffs, NJ (1979)
19. Glover, P.W.J., Matsuki, K., Hikima, R., Hayashi, K.: Characterising rock fractures using synthetic fractal analogues. Geotherm. Sci. Technol. **6** (1999)
20. GMSH website: http://www.geuz.org/gmsh/.
21. Grathwohl, P.: Diffusion in natural porous media: Contaminant Transport, Sorption/Desorption and Dissolution Kinetics. Kluwer Academic Publishers (2003)
22. Häfner, F., Sames, D., Voigt, H.-D.: Wärme- und Stofftransport – Mathematische Methoden. Springer, Berlin Heidelberg New York (1992)
23. Helmig, R., Braun, C., Manthey, S.: Upscaling of two-phase flow processes in heterogeneous porous media: determination of constitutive relationships. IAHS–AISH Publ. **277**, 28–36 (2002)
24. Istok, J.: Groundwater Modeling by the Finite Element Method. Water Resources Monograph. American Geophysical Union, Washington, DC (1989)
25. Kalbacher, T., Wang, W., McDermott, Ch., Kolditz, O., Taniguchi, T.: Development and application of a CAD interface for fractured rock. Environ. Geol. **47**, 1017–1027 (2005)
26. Kolditz, O.: Computational Methods in Environmental Fluid Mechanics. ISBN 3-540-42895-x. Berlin: Springer-Verlag, ss378 (2002).
27. Kolditz, O., Bauer, S.: A process-orientated approach to compute multi-field problems in porous media. Int. J. Hydroinf. **6**, 225–244 (2004)
28. Kolditz, O., Beinhorn, M., de Jonge, J., Xie, M., Kalbacher, T., Bauer, S.,Wang, W., Bauer, S., McDermott, C., Chen, C., Beyer, C., Gronewold, J., Kemmler, D., Legeida, D., Walsh, R., Du, Y.: GeoSys/RockFlow, open source software design. Technical Report, GeoSys-Preprint [2004-25] http://www.uni-tuebingen.de/zag/geohydrology. GeoSysResearch, Center for Applied Geosciences, University of Tübingen (2004)
29. Kosakowski, G.: Modellierung von Strömungs- und Transportprozessen in geklüfteten Medien: Vom natürlichen Kluftsystem zum numerischen Gitternetzwerk. VDI Fortschritt-Berichte **7**(304) (1996)
30. Kosakowski, G., Kasper, H., Taniguchi, T., Kolditz, O., Zielke, W.: Analysis of groundwater flow and transport in fractured rock – geometric complexity of numerical modelling. Z. Angew. Geol. **43**(2), 81–84 (1997)
31. Kosakowski, G., Berkowitz, B., Scher, H.: Analysis of field observations of tracer transport in a fractured till. J. Contam. Hydrol. **47**, 29–51 (2001)
32. Lauwerier, H.A.: The transport of heat in an oil layer caused by the injection of hot fluid. Appl. Sci. Res. **A5**, 145–150 (1955)
33. Louis, C.: Strömungsvorgänge in klüftigen Medien und ihre Wirkung aus die Standsicherheit von Bauwerken und Böschungen im Fels. Dissertation thesis, Universität Karlsruhe, Karlsruhe (1967)
34. Lunati, I., Kinzelbach, W., Sørensen, I.: Effects of pore volume–transmissivity correlation on transport phenomena. J. Contam. Hydrol. **67**, 195–217 (2003)
35. MAFIC (http://fracman.golder.com/software/mafic.asp).
36. Maloszewski, P., Zuber, A.: Tracer experiments in fractured rocks: matrix diffusion and the validity of models. Water Resour. Res. **29**, 2723–2735 (1993)
37. Maryška, J., Severýn, O., Vohralík, M.: Numerical simulation of fracture flow with a mixed-hybrid FEM stochastic discrete fracture network model. Comput. Geosci. **8**, 217–234 (2004)

38. McDermott, C.I., Kolditz, O.: Geomechanical model for fracture deformation under hydraulic, mechanical and thermal loads. Hydrogeol. J., Springer-Verlag, ISSN: 1431-2174 (Paper) 1435-0157 (Online) Doi: http://dx.doi.org/10.1007/s10040-005-0455-4 (2005)
39. McDermott, C.I., Lodemann, M., Ghergut, I., Tenzer, H., Sauter, M., Kolditz, O.: Investigation of coupled hydraulic–geomechanical processes at the KTB site: pressure dependent characteristics of a long term pump test and elastic interpretation using a geomechanical facies model. Geofluids **6**, 1–15 (2006)
40. Mettier, R., Kosakowski, G., Kolditz, O.: Influence of small scale heterogeneities on contaminant transport in fractured crystalline rock, Ground Water, submitted (2006)
41. Moreno, L., Tsang, Y.W., Tsang, C.F., Hale, F.V., Neretnieks, I.: Flow and tracer transport in a single fracture – a stochastic-model and its relation to some field observations. Water Resour. Res. **24** (12), 2033–2048 (1988)
42. Mourzenko, V.V., Thovert, J.-F., Adler, P.M.: Macroscopic permeability of three-dimensional networks with power-law size distribution. Phys. Rev. E **69** (2004)
43. National Research Council: Rock Fractures and Fluid Flow – Contemporary Understanding and Applications. Washington, DC: National Academy, 1996, ISBN:0-309-04996-2 (1996)
44. Neretnieks, I.: A Note on fracture flow dispersion mechanisms in the ground. Water Resour. Res. **19**(2), 364–370 (1983)
45. Oron, A.P., Berkowitz, B.: Flow in rock fractures: the local cubic law assumption reexamined. Water Resour. Res. **34**, 2811–2825 (1998)
46. Pebesma, E.J., Wesseling, C.G.: Gstat: a program for geostatistical modelling, prediction and simulation. Comput. Geosci. **24**(1), 17-31 (1998) http://www.gstat.org
47. Peratta, A., Popov, V.: A new scheme for numerical modelling of flow and transport processes in 3D fractured porous media. Adv. Water Resour. **29**, 42–61 (2005)
48. R Development Core Team: R: A Language and Environment for Statistical Computing. R Foundation for Statistical Computing, Vienna, Austria, ISBN 3-900051-07-0, http://www.R-project.org (2005)
49. Shewchuk, J.R.: Triangle: Engineering a 2D quality mesh generator and Delaunay triangulator. In: Ming, C., Manocha, L., Manocha, D.(eds.) Applied Computational Geometry: Towards Geometric Engineering, vol. 1148 of Lecture Notes in Computer Science, pp. 203–222. Springer, Berlin Heidelberg New York (1996)
50. Tsang, C.F.: Coupled hydromechanical–thermochemical processes in rock fractures. Rev. Geophys. **29**(4), 537–552 (1991)
51. Tsang, Y.W., Tsang, C.F.: Channel model of flow through fractured media. Water Resour. Res. **23**(3), 467–479 (1987)
52. Wang, J.S.Y., Narasimhan, T.N., Scholz, C.H.: Aperture correlation of a fractal fracture. J. Geophys. Res. **93**(B3), 2216–2224 (1988)
53. Wang, W., Kolditz, O.: Object-oriented finite element analysis of thermo-hydro-mechanical (THM) problems in porous media. Int. J. Numer. Methods Eng. (accepted) (2005)
54. Watson, D.F.: Computing the *n*-dimensional Delaunay tessellation with application to Voronoi polytopes. Comput. J. **24**(2), 167–172 (1981)
55. Witherspoon, P.A., Wang, J.S.Y., Iwai, K., Gale, J.E.: Validity of cubic law for fluid flow in a deformable rock fracture. Water Resour. Res. **16**(6), 1016–1024 (1980)
56. Zienkiewicz, O.C., Taylor, R.L.: The Finite Element Method, 1. Butterworth-Heinemann, 752 pp (2005)